

Z. YANG<sup>1,2\*</sup>, W. LIANG<sup>2</sup>, L. HU<sup>2,3</sup>, H. WANG<sup>1</sup>

## TRIBOLOGICAL BEHAVIORS OF OXYNITRIDE COATING ON TC4 ALLOY PREPARED BY DOUBLE GLOW TECHNOLOGY

The oxynitride coating was fabricated on the surface of Ti6Al4V alloy via double glow plasma alloy technology to enhance the wear resistance. The protective coating is dense and homogeneous and has a multilayer structure (outermost oxygen-rich layer, middle nitrogen-rich layer, innermost nitrogen diffusion layer). The acoustic emission curve suggests that the critical load is 53.1 N, the bonding strength between oxynitride coating and substrate is adequate to the application due to the diffusion layer. The oxynitride coating has a maximum hardness about 1020 HV, which is significant harder than Ti6Al4V alloy (370 HV). Tribological behaviors of oxynitride coating were investigated at three loads. The results indicated that the friction coefficient of oxynitride coating is lower than that of substrate at the same conditions. The wear mechanism of oxynitride coating is mainly fatigue wear, which converts to adhesive wear and fatigue wear with increasing load. The protective layer can decrease the actual contact areas obviously during the wear tests, which attributed to the higher hardness and stability of oxynitride layer.

*Keywords:* Double glow plasma technology; Oxynitride coating; TiC4 alloy; Tribological behavior; Diffusion

### 1. Introduction

Ti6Al4V alloys as engineering materials have been widely used in many industrial fields (such as aircraft components, chemical and food industries, biomedical applications), which attribute to the excellent properties of low elastic modulus, acceptable biocompatibility, high corrosion resistance and great mechanical properties of it [1-3]. In addition, titanium alloys are popular for demanding applications due to their excellent strength-to-weight ratio [4,5]. However, titanium alloys are limited to generalize because of the low hardness and poor wear resistance [6].

Many pieces of research were carried out to focus on the hardness or wear resistance of titanium alloys. W. Pawlak et al. [7] fabricated WC<sub>1-x</sub>/C coating on Ti-6Al-4V titanium alloy to enhance the wear resistance. Lu et al. [8] formed the Cr-Si co-alloyed coating on TA15 alloy can improve the tribological behavior. Even though these hard layers benefit the wear resistance, the protective coating easily peels off due to the apparent interface between the coating and substrate. However, titanium alloys have a high affinity to the oxygen or nitrogen element, which can easily form a hard layer consisting of Ti-N or Ti-O

compounds. The oxygen or nitrogen can cause diffusion into the surface of titanium alloys to enhance the wear resistance [9,10]. The protective coating has great bonding strength due to the diffusion treatment. For example, the hard layer consisting of TiN and Ti<sub>2</sub>N compounds was formed on the material surface after nitriding treatment [11]. After oxidizing treatment, TiO<sub>x</sub> compounds formed on the material surface to improve the wear resistance of the sample [12]. The oxynitriding treatment was through the formation of oxynitrides TiN<sub>x</sub>O<sub>1-x</sub>, and the protective coating of oxynitriding treatment was more complicated than that of nitriding or oxidizing treatment. Jiqiang Wu et al. [13] compared the nitriding, oxynitriding and carbonitriding treatments to improve the wear resistance of alloy, and the sample of oxynitriding treatment had the lower wear volumes among these techniques. Furthermore, the oxynitrides of titanium are popular in chemical or medical industrial fields because of their great mechanical and chemical properties [14].

Nowadays, many techniques have been used to fabricate oxynitride coating on titanium alloys, such as ion-plasma, diffusion and laser and high-energy methods etc [15]. Double glow plasma surface alloy technology is a new way of surface modification technology, called Xu-Tec [16]. Double glow technology has

<sup>1</sup> ANYANG INSTITUTE OF TECHNOLOGY, SCHOOL OF MECHANICAL ENGINEERING, WEST SECTION OF YELLOW RIVER AVENUE, ANYANG 455000, CHINA

<sup>2</sup> NANJING UNIVERSITY OF AERONAUTICS AND ASTRONAUTICS, SCHOOL OF MATERIALS SCIENCE AND TECHNOLOGY, 29 GENERAL AVENUE, NANJING 211100, CHINA

<sup>3</sup> NANJING IRON AND STEEL CO. LTD, SPECIAL STEEL DIVISION, XIEJIADIAN, LIUHE DISTRICT, NANJING 211100, CHINA

\* Corresponding author: 438099980@qq.com



been applied successfully to fabricate coatings such as N, C, Cr, Mo etc. [17] The double glow discharge produces a remarkable plasma region. The substrate surface is activated because of the bombardment by argon ions with high kinetic energy, which is advantageous to the diffusion of a beneficial element. The beneficial elements gain kinetic energy due to the glow discharge, which hits the surface of the substrate because of the force of the electric field [18]. The double glow technique has unique advantages, which could save precious metal resources and not cause pollution to the environment [19-21].

In this work, the specimens of Ti6Al4V alloys were subjected to oxynitriding treatment via double glow plasma surface alloy technology. The microstructure, bonding strength and wear behaviors of the oxynitride coating on Ti6Al4V alloy were investigated. The wear mechanism of the oxynitride layer was analyzed at 130 g, 230 g, and 330 g, respectively. The primary purpose of this work is to reveal the tribological characteristic of oxynitride coating fabricated by the double glow treatment.

## 2. Experiment

The substrate material in this work was Ti6Al4V alloy provided by the Beijing Iron and Steel Research Institute of China. The chemical composition of Ti6Al4V alloy is listed in TABLE 1. The specimens of Ti6Al4V alloys were cut into 15 mm × 15 mm × 5 mm rectangles by wire cutting. The specimens were polished with 1200 mesh water proof abrasive paper and cleaned in alcohol to expel the surface contamination by ultrasound equipment before they went through the experiment.

TABLE 1

The chemical composed of Ti6Al4V alloy (wt.%)

Ti	Al	V	Fe	O	C	N	H
Bal	5.5-6.8	3.5-4.5	≤0.3	≤0.2	≤0.1	≤0.05	≤0.015

The oxynitride coating was fabricated via double glow plasma surface alloy technology. The target used during the experiment process was 99.99 wt.% pure Ti with a diameter of 90 mm. Argon was used as background gas, and the flow ratio of argon, oxygen, and nitrogen was 9:1:8. The inside pressure of the furnace was 35 Pa, and the distance between the target and the substrate was 15 mm. The work piece voltage was 450 V, and the target voltage was 800 V. The preparation lasted three hours, and the processing temperature ranged from 800-900°C.

The microstructure of oxynitride coating were detected by scan electron microscopy (FEI, Quanta450, USA). The bonding strength between the oxynitride coating and the substrate was calculated by a scratch tester (BangYi, WS-2005, China), which has a diamond indenter with a speed of 1 mm min<sup>-1</sup>. The load rate was 25 N min<sup>-1</sup>, and the maximum load was 100 N. The crystal phase composition of oxynitride coating was investigated by X-ray diffraction (Rigaku, DMAX-RB12KW, Japan) with copper K $\alpha$  radiation ( $\lambda = 1.5418 \text{ \AA}$ ,  $20^\circ \leq 2\theta \leq 90^\circ$ ).

The microhardness of oxynitride coating was detected by Vickers Indenter (DianYing, DHV-1000/Z, China) with the applied load of 10 g for 15 s. The tribological behaviors of specimens with oxynitride coating were investigated by ball-on-disk friction and wear tester (KaiHua, HT-500, China) under dry sliding against GCr15. The tests were performed in air with a relative humidity of (45±5)%, the rotating rate was 560 rpm, and the turning radius was 2 mm. The testing temperature was 20°C at the load of 130 g, 230 g, and 330 g, respectively. The wear volumes were detected by depth-of-field system (Keyence, VHX-1000, Japan).

## 3. Results and discussion

### 3.1. Oxynitride Coating characterization

Fig. 1 reveals the microstructure of oxynitride coating on Ti6Al4V alloy. The results indicated that the surface of oxynitride coating is homogeneous and dense. There are no apparent holes or cracks in it. Fig. 1b is the magnified surface topography of oxynitride coating, and the SEM image indicated that very shallow pits appear on the coating surface, and lots of submicron crystalline grains are scattered on the coating surface. The reason can attribute to the characteristic of double glow technology. During the processing treatment, Ti elements were sputtered from the target and deposited on the substrate surface, the substrate surface was subjected to plasma bombardment to activate the substrate surface. Very shallow pits appeared on the surface due to plasma bombardment of the deposited layer.

Cross-section morphology of oxynitride coating (see Fig. 1c) and the EDS result (see Fig. 1d) indicated that the total thickness of oxynitride coating is 10.2  $\mu\text{m}$ , which is dense and without obvious defects on it. The oxynitride coating consists of an outermost oxygen-rich layer, a middle nitrogen-rich layer and an innermost nitrogen diffusion layer, which attributes to the difference in the flow ratio of oxygen and nitrogen. In addition, the bombardment of ions with a specific high kinetic energy also effects on the multilayer structure of oxynitride coating. During the treatment process, the oxygen and nitrogen elements were sputtered on a substrate surface, which diffused into the substrate due to the high treatment temperature. The interfaces between the outermost oxygen-rich layer, the middle nitrogen-rich layer and the innermost nitrogen diffusion layer are blurred due to the element diffusion at high treatment temperature according to the law of diffusion, which is beneficial to the bonding strength between oxynitride coating and substrate.

Fig. 2 shows the XRD pattern of oxynitride coating and the angle is 20° to 90°. The XRD results suggest that the main phases of protective coating are TiO<sub>2</sub>, TiN and Ti<sub>3</sub>N<sub>2-x</sub>, and a few TiO, Ti<sub>6</sub>O and Ti<sub>2</sub>N also formed during the treatment process. The results analyzed with EDS (see Fig. 1d) indicate that the phase formation of TiO<sub>2</sub> or TiN is favorable when the content of oxygen or nitrogen is high. In the diffusion area, the TiO and Ti<sub>6</sub>O phases formed due to the low content of oxygen or nitrogen element.

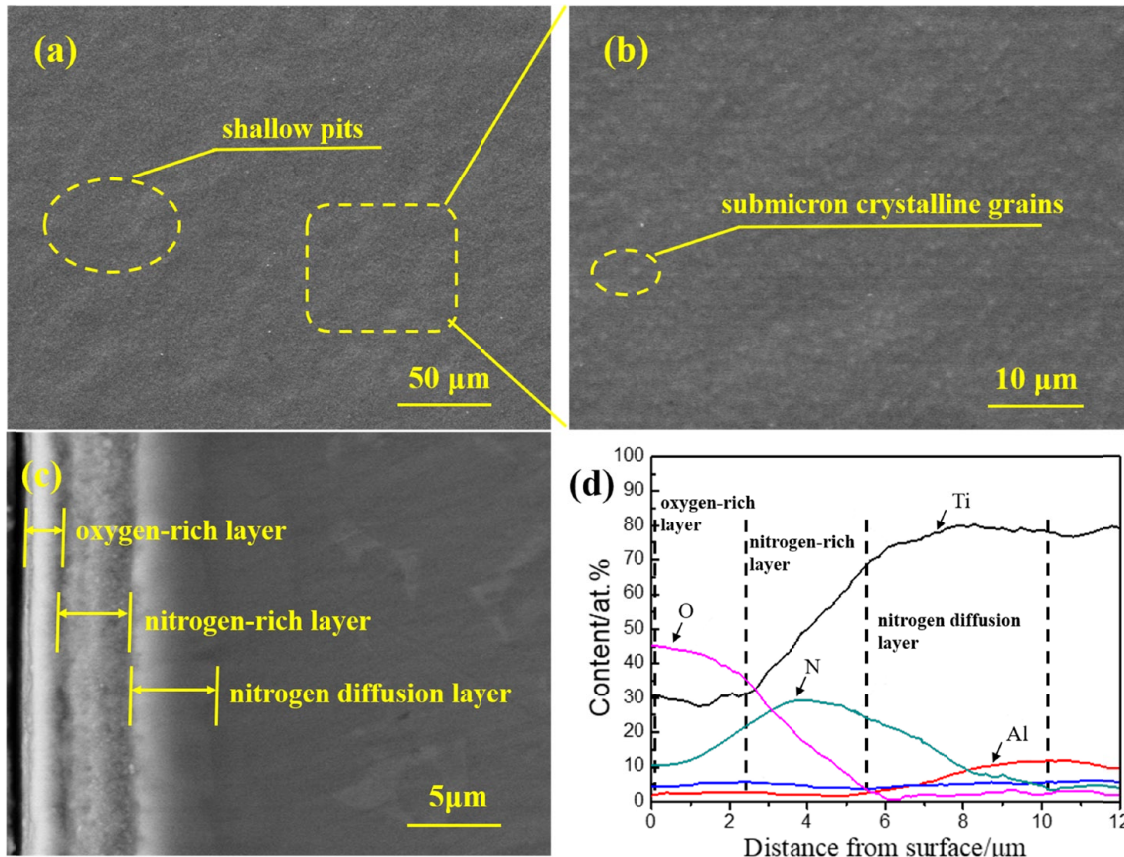


Fig. 1. SEM images of oxynitride coating (a) surface image, (b) magnified surface topography, (c) cross-section image (d) EDS result

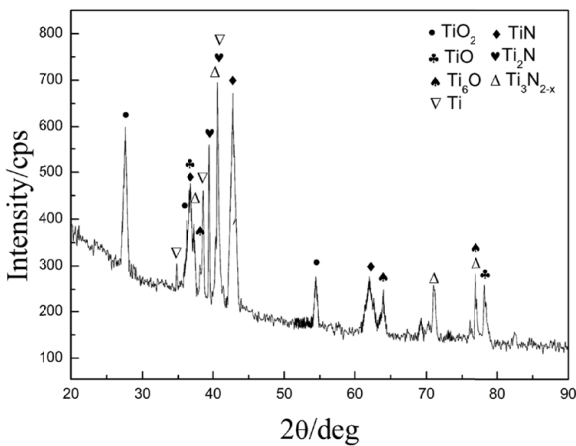


Fig. 2. XRD pattern of oxynitride coating

The microhardness profile of oxynitride coating shows in Fig. 3. The results suggested that the protective coating was significant harder than Ti6Al4V alloy, which had a maximum hardness about 1020 HV. The hardness of oxygen and nitrogen rich layer was in the range from 970 to 1020 HV. As the depth increased, the hardness value decreased rapidly until to the substrate, and the hardness of substrate was about 370 HV. Based on XRD and ESD results, the microhardness results indicated that the oxynitride coating could enhance the hardness effectively due to the formation of the nitrides and oxides on the surface of sample. The atoms of oxygen and nitrogen diffused

into Ti phase caused the crystal lattice distortion, which lead to precipitation hardening and then prevented the movement of dislocation. As for the nitrogen-diffusion layer, the nitride concentration decreased with increasing the depth, which lead to a sharp decrease in hardness.

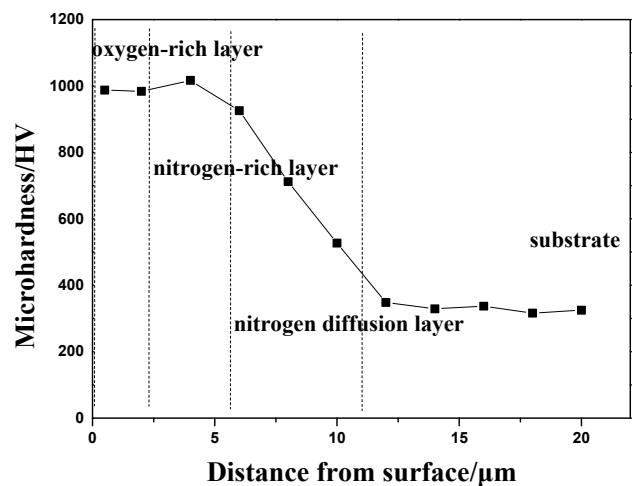


Fig. 3. Microhardness distributions of oxynitride coating

The availability of oxynitride coating was determined by the bonding strength between the protective coating and substrate during the coating service. The strength between the oxynitride coating and substrate was calculated by the WS-2005 scratch

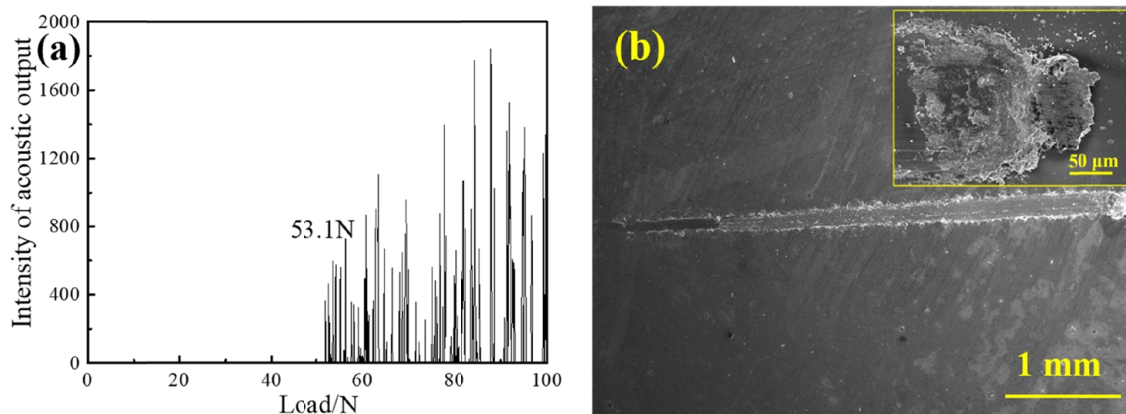


Fig. 4. Scratch test of oxynitride coating (a) acoustic emission curve, (b) image of scratch

tester. Fig. 4a shows the acoustic emission curve of oxynitride coating, which suggests that the bonding strength between the protective layer and the substrate is 53.1 N. When the microcracks appeared in the coating during the indenter drawn on the surface of the sample, an acoustical signal was produced and translated into a curve by an acoustic emission sensor. The results analyzed with surface microstructure (see Fig. 4b) indicate that the breadth or deepness of scratch changes uniformly. The scratch was slightly smooth, the plastic deformation appeared on the both sides of the scar. When the critical load was reached, microcracks appeared at the crystal boundary on the coating side boundary and began to expand, which led to the acoustical signal being produced. The bonding strength between the oxynitride coating and substrate is larger than 50 N, which is universally adequate for application [22,23].

### 3.2. Tribological behaviors

To evaluate the wear resistance of the oxynitride coating, a ball-on-disk friction and wear tester was used to investigate tribological behaviors of protective coating and substrate. Fig. 5 shows the friction coefficients of oxynitride coating and substrate against the GCr15 ball at normal temperatures under 130 g, 230 g and 330 g. The results indicated that the friction coefficients of

Ti6Al4V alloy (see Fig. 5a) increased rapidly at the early stage during the wear tests. The friction coefficients remained stable after 3 min, and the values of friction coefficients of the substrate were stable at 0.3-0.7. The friction coefficient curves of the substrate fluctuated obviously, which attribute to the production of abrasive dust between the GCr15 ball and the substrate surface during the wear process. The load during the wear tests affected the average friction coefficients of Ti6Al4V alloy.

Fig. 5b shows the friction coefficients of oxynitride coating. The results suggested the values of friction coefficients were much lower than that of the substrate, which was stable at 0.3-0.42. The average friction coefficients of protective coating also increased slightly with increasing load. Compared with the results of Fig. 5a and Fig. 5b, the change of friction coefficients of oxynitride coating and substrate was related to the hardness of the surface. Previous studies [20] suggested that the specimen with higher surface hardness led to a lower friction coefficient. During the wear tests, the  $\text{TiO}_2$ ,  $\text{TiO}$ ,  $\text{TiN}$  and  $\text{Ti}_2\text{N}$  etc., with the high hardness, reduced the genuine contact parts against the friction pair.

Fig. 6 shows the 3D profiles of wear tracks of oxynitride coating and substrate at 130 g, 230 g, and 330 g, respectively. The results indicated that the width and depth of wear tracks of the protective layer and substrate became more significant with increasing load. In addition, the areas of wear tracks of oxynitride coating were smaller than that of the substrate obviously.

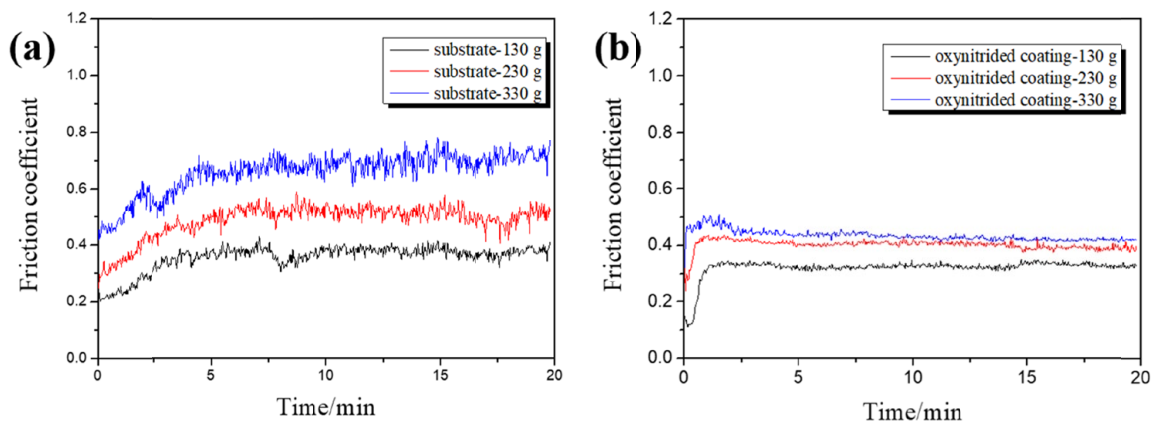


Fig. 5. friction coefficients against GCr15 ball with 130 g, 230 g and 330 g load (a) substrate, (b) oxynitride coating

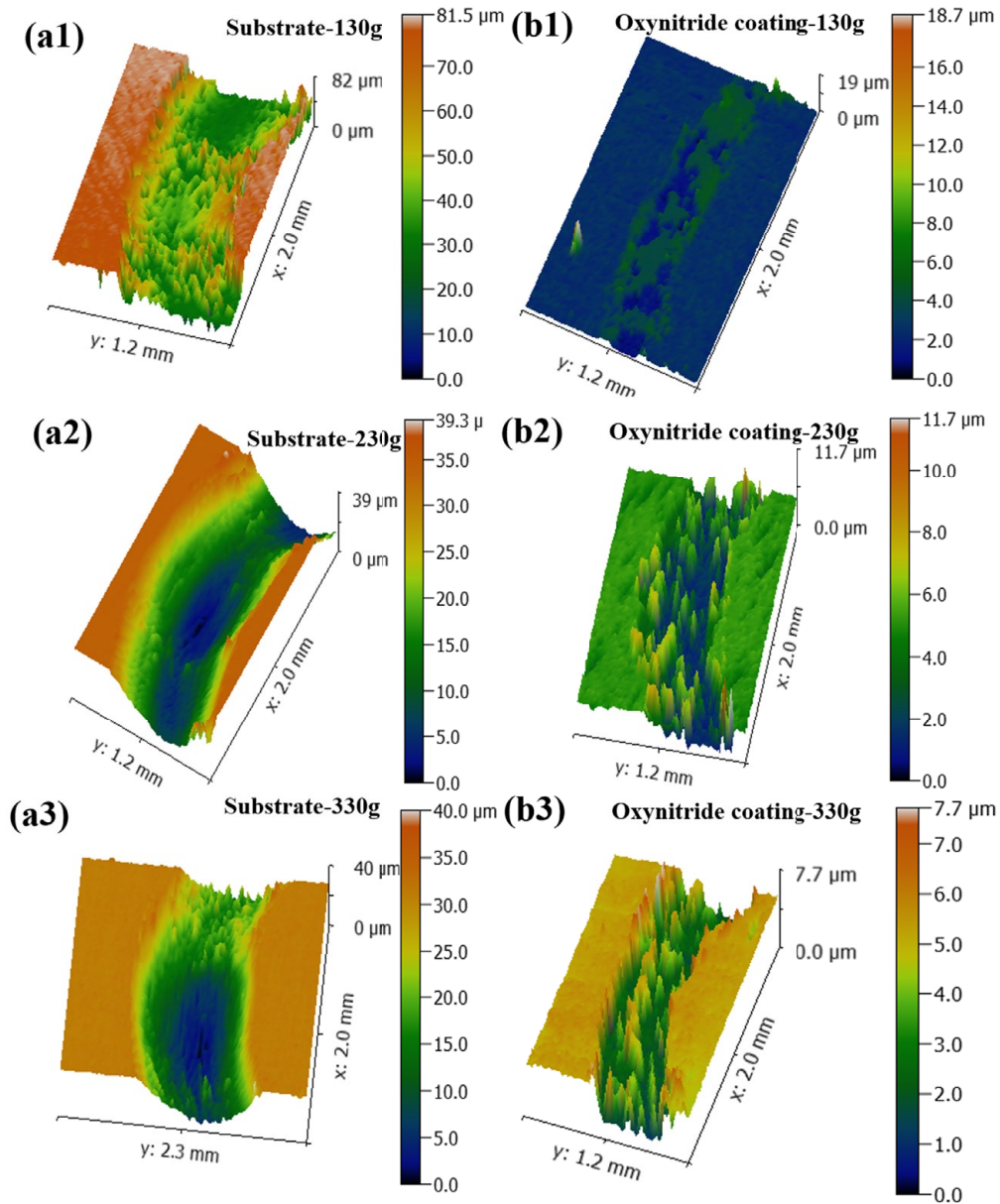


Fig. 6. the surface profile of wear tracks (a) substrate, (b) oxynitride coating

The wear results of oxynitride coating and substrate were calculated from the surface profile, which was listed in TABLE 2. To evaluate the wear resistance of specimens, the wear volume was calculated by the following equation [8].

$$V = \frac{2\pi hr}{6b} \cdot (3h^2 + 4b^2) \quad (1)$$

Where  $h$  is the depth of wear track,  $r$  is radius of wear track,  $b$  is the width of wear track,  $V$  is the volume of wear area.

$$v = \frac{V}{S} \quad (2)$$

$$K = \frac{V}{SP} \quad (3)$$

Where  $v$  represents wear rate,  $S$  is sliding distance,  $K$  represents specific wear rate,  $P$  represents the load.

The wear rate is determined by sliding distance and wear volume. The specific wear rate is the objective measure of wear properties. TABLE 2 suggests that the wear rate and specific wear rate increased as the load increased for oxynitride coating and substrate, respectively. However, the wear rate and specific wear rate of the protective coating were much lower than those of the substrate under the same load condition. The results indicate that the oxynitride coating fabricated on Ti6Al4V alloy can significantly improve wear properties, which attributes to the higher surface hardness of the protective layer. The oxynitride coating has higher hardness than the substrate due to the formation of the oxide or the nitride of the titanium in the coating. During the wear treatment, the substrate suffered considerable wear than oxynitride coating on the sample surface. The protective coating reduced the genuine contact parts against the friction pair, and specific wear rates and wear rates of oxynitride coating were smaller than that of substrate obviously.

Wear results of oxynitride coating and Ti6Al4V substrate

Specimens	Width $b/\text{mm}$	Depth $h/\mu\text{m}$	Volume loss $V/10^{-3}\text{mm}^3$	Wear rate $v/10^{-4}\text{mm}^3\text{m}^{-1}$	Specific wear rate $K/10^{-5}\text{mm}^3\text{N}^{-1}\text{m}^{-1}$
Ti6Al4V Substrate-130 g	0.74	20	124.45	8.30	65.14
Ti6Al4V Substrate-230 g	0.93	30	233.80	15.59	69.15
Ti6Al4V Substrate-330 g	1.09	37.9	346.86	23.12	71.50
Oxynitride Coating-130 g	0.24	0.8	1.65	0.11	0.86
Oxynitride Coating-230 g	0.51	2.7	11.41	0.76	3.38
Oxynitride Coating-330 g	0.78	2.72	17.72	1.18	3.65

### 3.3. Tribological mechanism

Fig. 7 shows the magnified surface topography of wear tracks of oxynitride coating and substrate under the load of 130 g, 230 g, and 330 g, respectively. For substrate, neatly arranged furrows were produced on the wear surface, and lots of particles appear randomly on the surface. This phenomenon suggested that

the wear mechanism was dominated by abrasive wear. As the load increased to 230 g, a few particles appeared on the wear track. Slight delamination occurred at the edge of the furrow, suggesting abrasive and slightly adhesive wear features. With the load increased to 330 g, the depth of furrows was reduced, the adhesion transfer could be observed, and a number of abrasive particles appeared on the wear surface. The wear mechanism was abrasive

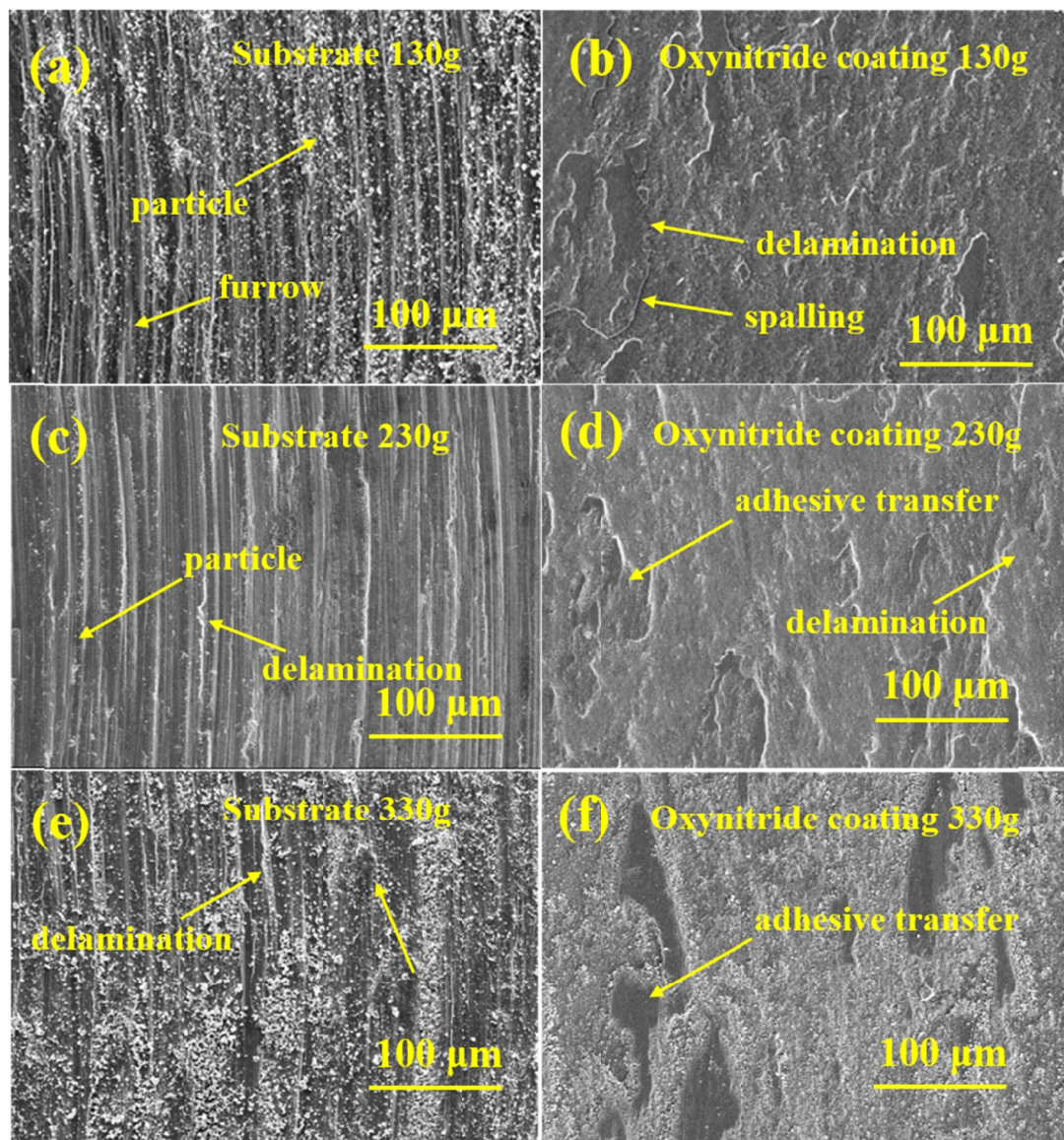


Fig. 7. Wear morphology of wear track at 130 g, 230 g and 330 g load, respectively (a, c and e) substrate, (b, d and f) oxynitride coating

wear and adhesive wear. The wear morphology of the substrate suggested that wear resistance of Ti6Al4V alloy was poor due to the low surface hardness. Fig. 7b, d, and f show the wear surface of oxynitride coating at 130 g, 230 g, and 330 g, respectively. Compared with the substrate, the deformation of oxynitride coating is much lower, which attribute to the higher hardness of the protective coating. Under the 130 g load, plastic deformation and large area spalling appeared on the wear track, which suggested the wear mechanism was mainly fatigue wear. With the load increased, a more severe phenomenon of plastic deformation and adhesive transfer appeared on the wear surface, which suggested the wear mechanism was adhesive wear and fatigue wear. Above all, the wear of oxynitride coating was much weaker than that of the substrate. And wear surface of the protective coating had not been damaged seriously, which attribute to the higher hardness and stability of oxynitride layer. This indicated that the oxynitride coating effectively improves the wear resistance of Ti6Al4V alloy.

#### 4. Conclusion

The oxynitride coating was fabricated on Ti6Al4V alloy via the double glow plasma surface alloy technology to improve the wear resistance. The results indicated that the oxynitride coating had a multilayer structure, consisting of an outermost oxygen-rich layer, a middle nitrogen-rich layer and an innermost nitrogen diffusion layer. The protective coating was homogeneous and dense. The main phases of  $\text{TiO}_2$ , TiN and  $\text{Ti}_3\text{N}_{2-x}$  were formed during the double glow treatment, which related to the content of oxygen or nitrogen element. The microhardness of oxynitride coating was in the range from 970 to 1020 HV, which was much higher than that of substrate (about 370 HV). The bonding strength between the protective coating and substrate was 53.1 N and universally adequate to application, attributed to the diffusion of oxygen or nitrogen element.

The friction coefficients of oxynitride coating were much lower than that of the substrate under the same load conditions. The primary wear mechanism of Ti6Al4V alloy was abrasive wear, which transformed to adhesive wear with the load increased. The wear mechanism of oxynitride coating was mainly fatigue wear, which converted to adhesive wear and fatigue wear with increasing load. The wear of oxynitride coating was much weaker than that of the substrate. And the wear surface of protective coating had not been damaged seriously, which attribute to the higher hardness and stability of the oxynitride layer. The protective coating can obviously decrease the actual contact areas during the wear tests.

#### Acknowledgments

This project was supported by the National Natural Science Foundation of China (No.51874185), the Anyang Science and Technology Planning Project (No.2022C01GX010), and the Doctoral Fund of Anyang Institute of Technology (No.BSJ2022030)

#### REFERENCES

- [1] Shunyu Liu, Yung C. Shin, Additive manufacturing of Ti6Al4V alloy: A review. *Mater. Des.* **164**, 107552 (2019). DOI: <https://doi.org/10.1016/j.matdes.2018.107552>
- [2] A. Eakambaram, M. Anthony Xavier, Influence of recast layer on the fatigue life of Ti6Al4V processed by electric discharge machining. *Arch. Metall. Mater.* **64**, 1541-1548 (2019). DOI: 10.24425/amm.2019.130124
- [3] Andrew H. Chern, Peeyush Nandwana, Tao Yuan, Michael M. Kirka, Ryan R. Dehoff, Peter K. Liaw, Chad E. Duty, A review on the fatigue behavior of Ti-6Al-4V fabricated by electron beam melting additive manufacturing. *Int. J. Fatigue* **119**, 173-184 (2019). DOI: <https://doi.org/10.1016/j.ijfatigue.2018.09.022>
- [4] X. Chen, F.Q. Xie, T.J. Ma, W.Y. Li, X.Q. Wu, Effects of post-weld heat treatment on microstructure and mechanical properties of linear friction welded  $\text{Ti}_2\text{AlNb}$  alloy. *Mater. Des.* **94**, 45-53 (2016). DOI: <http://dx.doi.org/10.1016/j.matdes.2016.01.017>
- [5] Peter C. King, Christian Busch, Teresa Kittel-Sherri, Mahnaz Jahedi, Stefan Gulizia, Interface melting in cold spray titanium particle impact. *Surf. Coat. Technol.* **239**, 191-199 (2014). DOI: <https://doi.org/10.1016/j.surfcoat.2013.11.039>
- [6] O.I. Yaskiv, I.M. Pohrelyuk, V.M. Fedirko, Dong Bok Lee, O.V. Tkachuk, Formation of oxynitrides on titanium alloys by gas diffusion treatment. *Thin Solid Films* **519** (19), 6508-6514 (2011). DOI: <https://doi.org/10.1016/j.tsf.2011.04.219>
- [7] W. Pawlak, K.J. Kubiak, B.G. Wendler, T.G. Mathia, Wear resistant multilayer nanocomposite  $\text{WC}_{1-x}/\text{C}$  coating on Ti-6Al-4V titanium alloy. *Tribol. Int.* **82**, 400-406 (2015). DOI: <https://doi.org/10.1016/j.triboint.2014.05.030>
- [8] H.F. Lu, W.P. Liang, Q. Miao, F. Wang, Z. Ding, J.J. Xia, High-temperature tribological behaviors of a Cr-Si co-alloyed layer on TA15 alloy. *Chin. J. Aeronaut.* **30** (2), 846-855 (2017). DOI: <https://doi.org/10.1016/j.cja.2016.10.020>
- [9] I. Pohrelyuk, J. Morgiel, O. Tkachuk, K. Szymkiewicz, Effect of temperature on gas oxynitriding of Ti-6Al-4V alloy. *Surf. Coat. Technol.* **360**, 103-109 (2019). DOI: <https://doi.org/10.1016/j.surfcoat.2019.01.015>
- [10] A.F. Yetim, F. Yildiz, Y. Vangolu, A. Alasaran, A. Celik, Several plasma diffusion processes for improving wear properties of Ti6Al4V alloy. *Wear* **267**, 2179-2185 (2009). DOI: <https://doi.org/10.1016/j.wear.2009.04.005>
- [11] Dong Bok Lee, Waheed Ali Abro, Kun Sang Lee, Muhammad Ali Abro, Iryna Pohrelyuk, Oleh Yaskiv, Gas Nitriding and Oxidation of Ti-6Al-4V Alloy. *Defect Diffus. Forum* **382**, 155-159 (2018). DOI: <https://doi.org/10.4028/www.scientific.net/DDF.382.155>
- [12] G. Cassar, J.C. Avelar-Batista Wilson, S. Banfield, J. Housden, A. Matthews, A. Leyland, Surface modification of Ti-6Al-4V alloys using triode plasma oxidation treatments. *Surf. Coat. Technol.* **206** (22), 4553-4561 (2012). DOI: <https://doi.org/10.1016/j.surfcoat.2012.05.001>
- [13] Jiqiang Wu, Han Liu, Jingcai Li, Xingmei Yang, Jing Hu, Comparative study of plasma oxynitriding and plasma nitriding for AISI 4140 steel. *J. Alloys Compd.* **680**, 642-645 (2016). DOI: <https://doi.org/10.1016/j.jallcom.2016.04.172>

- [14] Oleh Tkachuk, Iryna N. Pohrelyuk, Roman Proskurnyak, J. Guspel, E. Beltowska-Lehman, Jerzy Morgiel, Electrochemical Behavior of Ti–6Al–4V Alloy in Ringer’s Solution After Oxynitriding. *Mater. Sci.* **54** (4), 542-546 (2019). DOI: <https://doi.org/10.1007/s11003-019-00215-0>
- [15] I. M. Pohrelyuk, Oleh Tkachuk, Roman Proskurnyak, Nataliya Boiko, O. Yu. Kluchivska, R.S. Stoika, Piotr Ozga, Cytocompatibility Evaluation of Ti-6Al-4V Alloy After Gas Oxynitriding. *J. Mater. Eng. Perform.* **29** (12), 7785-7792 (2020). DOI: <https://doi.org/10.1007/s11665-020-05265-z>
- [16] Z.G. Yang, W.P. Liang, Y.L. Jia, Q. Miao, Z. Ding, Y. Qi, Corrosion behavior of double-glow plasma copperizing coating on Q235 steel. *J. Min. Metall., Sect. B* **56**, 257-268 (2020). DOI: <https://doi.org/10.2298/JMMB190820017Y>
- [17] Chen Xiaohu, Zhang Pingze, Wei Dongbo, Ding Feng, Li Fengkun, Wei Xiangfei, Ma Shijian, Preparation and characterization of Cr/CrC multilayer on  $\gamma$ -TiAl alloy by the double glow plasma surface alloying technology. *Mater. Lett.* **215**, 292-295 (2018). DOI: <https://doi.org/10.1016/j.matlet.2017.12.104>
- [18] S.Y. Cui, Q. Miao, W.P. Liang, B.Q. Li, Oxidation behavior of NiCoCrAlY coatings deposited by Double-Glow plasma alloying. *Appl. Surf. Sci.* **428**, 781-787 (2018). DOI: <https://doi.org/10.1016/j.apsusc.2017.09.215>
- [19] D.B. Wei, P.Z. Zhang, Z.J. Yao, X.F. Wei, J.T. Tang, X.H. Chen, Preparation and high-temperature oxidation behavior of plasma Cr–Ni alloying on ti6al4v alloy based on double glow plasma surface metallurgy technology. *Appl. Surf. Sci.* **388**, 571-578 (2016). DOI: <https://doi.org/10.1016/j.apsusc.2015.10.064>
- [20] Z.G. Yang, W.P. Liang, Q. Miao, Z. Ding, S.W. Zuo, Tribological behavior of borocarbured layer on low-carbon steel treated by double glow plasma surface alloying. *Mater. Res. Express* **5**, 046408 (2018). DOI: <https://doi.org/10.1088/2053-1591/ab9980>
- [21] Song Xu, Paul Munroe, Jiang Xu, Zonghan Xie, The microstructure and mechanical properties of tantalum nitride coatings deposited by a plasma assisted bias sputtering deposition process. *Surf. Coat. Technol.* **307**, 470-475 (2016). DOI: <https://doi.org/10.1016/j.surfcoat.2016.09.015>
- [22] D.B. Wei, H.X. Liang, S.Q. Li, F.K. Li, F. Ding, S.Y. Wang, Z.L. Liu, P.Z. Zhang, Microstructure and tribological behavior of W-Mo alloy coating on powder metallurgy gears based on double glow plasma surface alloying technology. *J. Min. Metall., Sect. B* **55**, 227-234 (2019). DOI: <https://doi.org/10.2298/JMMB181031022D>
- [23] Y. Xu, W. Liang, Q. Miao, Q. Jiang, B. Ren, Z. Yao, P. Zhang, D. Wei, High temperature oxidation behaviour of  $\text{Al}_2\text{O}_3/\text{Al}$  composite coating on  $\gamma$ -TiAl. *Surf. Eng.* **31** (5), 354-360 (2015). DOI: <http://dx.doi.org/10.1179/1743294414Y.0000000363>